Thermal-conductivity—reduced-state Correlation for the Inert Gases

E. JAMES OWENS and GEORGE THODOS

Northwestern Technological Institute, Evanston, Illinois

The fragmentary thermal-conductivity data for argon available in the literature have been correlated by use of a residual thermal conductivity $k - k^*$ vs. density ρ relationship. This correlation produced a unique continuous curve which was found to be singularly independent of temperature and pressure for both gaseous- and liquid-state data. From low-pressure thermal-conductivity values k^* and the relationship given above, it is possible to determine thermal conductivities at any condition of temperature and pressure for which a corresponding density is available. This procedure was used to calculate reliable thermal conductivities k for high-pressure regions where experimental data were lacking.

In a similar manner the critical thermal conductivity k_c for argon was established directly from the critical density and the quantity $k_{T_c}^*$. The k_c value permitted the calculation of reduced thermal conductivities k_R and made possible the construction of an extensive reduced-state chart. Although this correlation was developed mainly from data for argon, it was found to apply equally as well to the other inert gases as postulated from the theory of corresponding states.

A comparison of thermal conductivities calculated from the reduced-state plot with over 200 experimental points produced an average deviation of 1.8% for all the inert gases. This chart was also found applicable to the diatomic gases and their mixtures but produced significant deviations for substances having more than two atoms per molecule.

Present-day heat transfer studies require an exacting definition of the thermal properties of fluids over wide ranges of temperature and pressure. In general, the thermal properties of fluids can be obtained from reliable correlations already available in the literature (*5, 18, 43*); however, present methods do not permit the calculation of accurate thermal conductivities for both gases and liquids except over limited ranges of temperature and pressure. Thermal-conductivity values available in the literature are generally presented only for the more common substances and in most cases are restricted to the low-pressure region where P_R is essentially equal to zero. Relatively few experimental data are available for high pressures and for conditions approaching the critical point.

Existing theoretical methods (*8, 14, 34*) for estimating thermal conductivities are generally limited to the low-pressure region and cannot be used to predict accurate values for the liquid state. Similarly, theoretical equations (*15, 42*) are available for predicting the thermal conductivity of certain types of liquids, but these relationships cannot be applied to the gaseous state. Specific correlations are available for calculating the thermal conductivity of gases at high pressures (*7, 11, 32*); however, these methods require a considerable amount of experimental data or are restricted in application owing to questionable accuracy. In the present investigation (*39*) an attempt was made to overcome these limitations and to produce a method for calculating the thermal conductivity of both gases and liquids over wide ranges of temperature and pressure.

PREVIOUS DEVELOPMENTS

Early attempts to predict the thermal conductivity of gases have been based primarily upon kinetic theory. Most of these developments have been limited to the low-pressure region, where the mean free path of gas molecules is small in comparison to the dimensions of the system. This region is generally restricted to pressures ranging from 1 atm. to 10 mm. Hg.

Maxwell (*34*), Sutherland (*46*), and Eucken (*8*) have presented theoretical expressions to predict the thermal conductivity of some gases at low pressures with fair accuracy. Although these relationships are of classical interest, they are not applicable to the liquid state and fail to produce reliable thermal conductivities at high pressures and temperatures.

More recently Hirschfelder, Curtiss, and Bird (*14*) developed a relationship for predicting the thermal conductivity of monoatomic gases at low pressures. Using the concepts of statistical mechanics, these investigators derived the following equation for nonpolar gases:

$$k^* = 1.9891 \times 10^{-4} f_k \frac{\sqrt{T/M}}{\sigma^2 \Omega^{(2,2)*}[T_N]} \tag{1}$$

Equation (1) can also be applied to polyatomic gases if f_k (*14*) is replaced by the Eucken correction factor (*8*). This equation produces accurate thermal conductivity values at low pressures for many nonpolar gases for which the force constants ϵ and σ are available.

Using concepts of advanced kinetic theory, Enskog (*7*) derived an equation of state and expressions to predict the effect of pressure on the thermal conductivity and viscosity of nonpolar gases:

$$P + \alpha\rho^2 = \frac{RT}{M}\rho[1 + \beta\rho\chi] \tag{2}$$

$$\frac{\mu}{\mu^*} = \beta\rho\left[\frac{1}{\beta\rho\chi} + 0.7614\beta\rho\chi + 0.8\right] \tag{3}$$

$$\frac{k}{k^*} = \beta\rho\left[\frac{1}{\beta\rho\chi} + 0.7575\beta\rho\chi + 1.2\right] \tag{4}$$

in which it is assumed that α and β are constants and χ is a function of density only. In this development Enskog further assumed that multiple collisions between the gas molecules were negligible and that the molecules behaved as rigid elastic spheres which exerted attractive forces only. The basic derivation and use of the Enskog equations are clearly illustrated elsewhere (*16*).

Michels and Botzen (*35*) have found that these relationships are valid up to pressures of approximately 1,000 atm., where the basic assumptions of Enskog begin to break down. Equations (2), (3), and (4) are capable of producing reliable thermal conductivity and viscosity values when sufficient experimental data are available to define the values of α, β, and χ. This requirement limits the application of the Enskog expressions to systems having an extensive experimental background.

Nathan and Comings (*37*) used high-pressure viscosity and P.V.T. data for a number of gases to evaluate α, β, and χ

E. James Owens is at present with the California Research Corporation, Richmond, California.

Large reproductions of Figure 7 in sizes of 8½ by 11 and 11 by 13½ in. are available on request from the Chemical Engineering Department, Northwestern University, Evanston, Illinois.

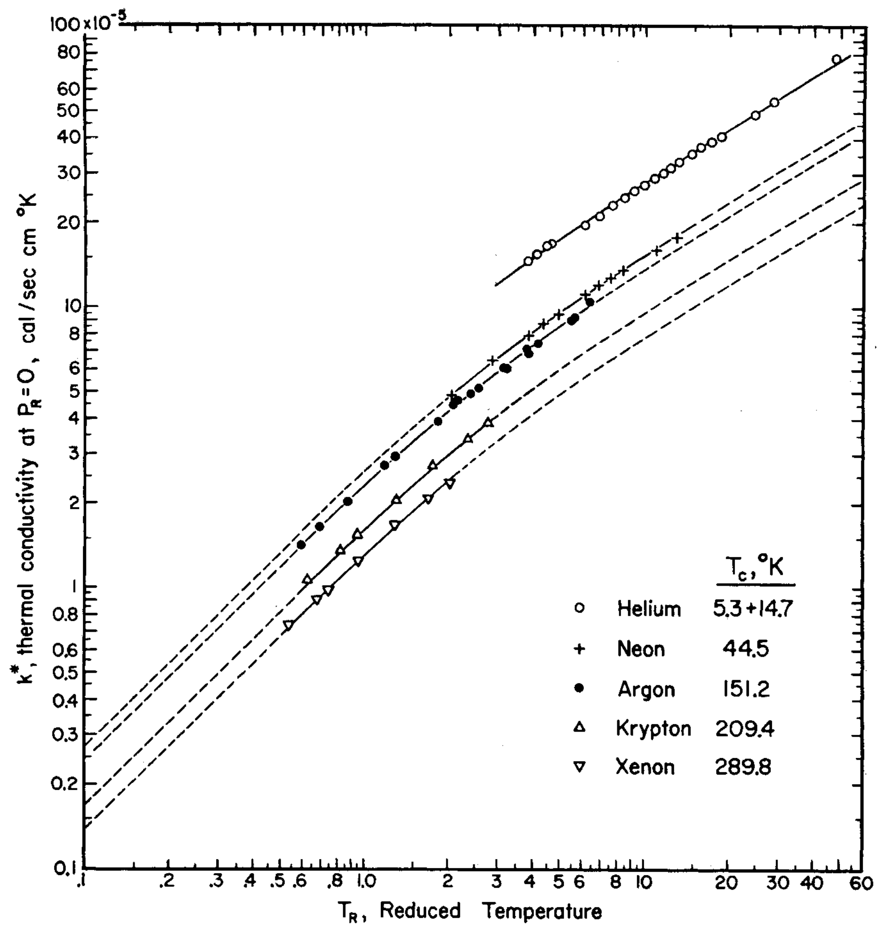

Fig. 1. Thermal-conductivity–reduced-temperature relationships for the inert gases at $P_R = 0$.

in the Enskog equations. Substituting these values into Equation (4) permitted the ratio k/k^* to be calculated directly and plotted as a generalized function of reduced temperature and pressure. This correlation was later revised by Lenoir, Junk, and Comings (*32*) to include data for several additional gases. The revised plot produces satisfactory thermal conductivities for many gases at conditions ranging from reduced temperatures of $T_R = 1$ to $T_R = 3$ and reduced pressures of $P_R = 0.6$ to $P_R = 7.5$. However, its general use is restricted to those substances for which k^* data may be either estimated (*8, 14, 34*) or obtained directly from the literature.

Gamson (*11*) has presented a more flexible correlation in which the reduced thermal conductivity k/k_c, rather than the ratio k/k^*, is plotted as a function of reduced temperature and pressure. Based on the Enskog equations and the work of Nathan and Comings (*37*), Gamson made the fundamental assumption that

$$\frac{k/k^*}{\mu/\mu^*} = f(T_R, P_R) \qquad (5)$$

Equation (5) can be expressed in terms of reduced conditions as

$$\frac{k_R}{\mu_R}\,\frac{\mu_R^*}{k_R^*} = f(T_R, P_R) \qquad (6)$$

A relationship for the thermal conductivity at the critical point was obtained by evaluating Equation (6) at the critical temperature and pressure where $k_R/\mu_R = 1$. The quantity μ_R^* was calculated from the reduced viscosity plot of Uyehara and Watson (*50*), and $f(T_R, P_R)$ was obtained from the work of Nathan and Comings (*37*) to produce

$$k_c = 2.60 k_{T_c}^* \qquad (7)$$

Using Equation (7), Gamson established a low-pressure reduced-thermal-conductivity curve based on the experimental data for over twenty-five substances. Reduced thermal conductivities at elevated pressures were calculated from Equation (6) by extrapolating the $f(T_R, P_R)$ values determined by Nathan and Comings. In this manner, a generalized reduced-state correlation was constructed to include reduced temperatures in the range from $T_R = 0.3$ to $T_R = 40$ and reduced pressures ranging from $P_R = 0$ to $P_R = 30$.

The accuracy of Gamson's correlation is open to speculation because it was produced from relatively few experimental data obtained in the low-pressure region. Furthermore, the validity of this plot above $T_R = 3.0$ and $P_R = 10.0$ is particularly questionable since an extensive extrapolation of the Nathan and Comings data was used to establish this entire region.

REDUCED-STATE CORRELATIONS

Generalized reduced-state plots are based on the validity of the theory of corresponding states as originally proposed by van der Waals (*51*). It is recognized that the classical form of this theory is only approximately true for all fluids. In order for all substances to conform to the behavior of a corresponding state, it would be necessary for them to have molecules of the same shape with similar intermolecular-force relationships. Since this requirement is not generally met, the classical theory should apply well only to members of a homologous series or to a family of substances which exhibit similar molecular behavior. A universal reduced-thermal-conductivity correlation would of necessity encompass substances of all types, and, therefore, significant errors may be inherent in this type of plot. The application of a reduced-state analysis to a family of similar substances should tend to eliminate such errors and to produce a more accurate correlation. Because of these advantages, the restricted rather than the universal approach was used in the following development.

DEVELOPMENT OF PRESENT METHOD OF CORRELATION

The inert gases have been arbitrarily selected as the basis for the present study. Experimental data for helium, neon, argon, krypton, and xenon have been obtained from the literature sources presented in Table 1.

The low-pressure thermal conductivities* for the inert gases have been plotted against reduced temperature on log-log scales to produce the curves presented in Figure 1. The low-temperature portion of these curves was obtained by extrapolating on rectilinear coordinates the available data to $k^* = 0$ when $T = 0$°K. The relationships of Figure 1 are found to be parallel and should be capable of translation into a single curve when the data are divided by the ordinate at any reduced temperature T_R, such as the thermal conductivity at the critical temperature.

The relationships shown in Figure 1 may be expressed analytically as

$$\log k^* = B \log T_R + \log C \qquad (8)$$

For a set of parallel curves such as that given in Figure 1, B becomes a function of reduced temperature only and is the same for all substances considered in this study. If Equation (8) is evaluated at $T_R = 1.0$, the constant C is defined as

$$C = k_{T_c}^* \qquad (9)$$

---

*Experimental k values measured at essentially atmospheric pressure, for which P_R is approximately equal to zero.

TABLE 1. SOURCES OF EXPERIMENTAL DATA

Source	Helium	Neon	Argon	Krypton	Xenon
3	X				
12	X				
19	X				
22	X	X	X	X	X
23		X	X		
24	X	X	X		
27		X	X		
28			X	X	X
31	X		X		
32			X		
41	X		X		
45	X		X		
47	X	X			
48	X				
49			X		
54			X		

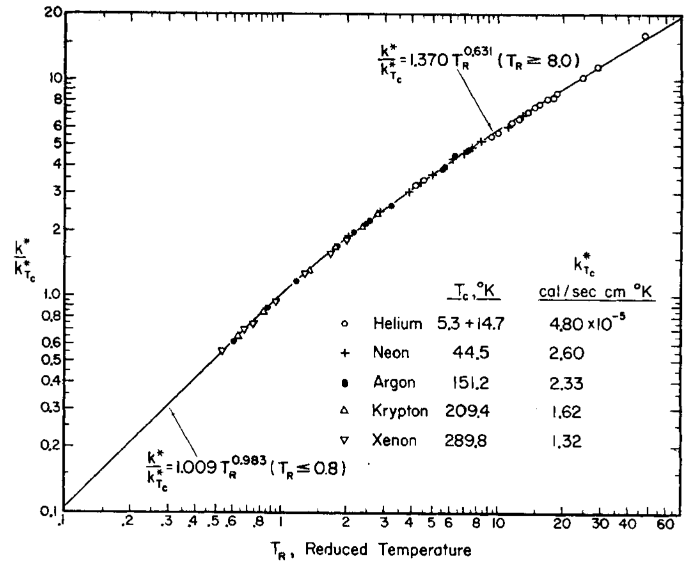

Fig. 2. Correlation of thermal-conductivity ratios for the inert gases at $P_R = 0$ (reference state: critical temperature and $P_R = 0$).

which, when substituted into Equation (8), produces

$$\log \frac{k^*}{k_{T_c}^*} = B \log T_R \qquad (10)$$

Equation (10) suggests that a single curve should result when the thermal conductivity ratio, $k^*/k_{T_c}^*$, is plotted against reduced temperature T_R on log-log coordinates. This behavior should follow for any family of similar substances which produce parallel curves on a plot of the type presented in Figure 1.

Values for the $k_{T_c}^*$ of neon, argon, krypton, and xenon were obtained directly from Figure 1. Thermal conductivity ratios, $k^*/k_{T_c}^*$, calculated from these quantities were plotted against reduced temperature to produce the single curve presented in Figure 2. The straight-line portions of this relationship are defined analytically by the following equations:

$$\frac{k^*}{k_{T_c}^*} = 1.009 T_R^{0.983} \quad \text{for} \quad T_R \leq 0.8 \qquad (11)$$

$$\frac{k^*}{k_{T_c}^*} = 1.370 T_R^{0.631} \quad \text{for} \quad T_R \geq 8.0 \qquad (12)$$

The curve in Figure 2 permitted the low-pressure data for each of the inert gases to be extrapolated over the entire reduced-temperature range covered by the $k^*/k_{T_c}^*$ ratios for all the gases. Accordingly, extrapolated values were calculated for neon, argon, krypton, and xenon and are indicated as the dashed portion of the curves presented in Figure 1.

Initially, the data for helium did not fall in line with the correlation presented in Figure 2. It has been shown (*6*) that this deviation from classical behavior can be explained and accounted for explicitly by the quantum-mechanical principle of corresponding states. However, in this study the helium data were fitted to the relationship of Figure 2 by replacing its true critical temperature of 5.3°K. with an arbitrary pseudocritical value of 20°K. This treatment is similar to that used for correcting the incongruous behavior of helium on other types of reduced-state correlations (*33, 38*).

An average $k_{T_c}^*$ value for helium was determined from Figure 2 by use of pseudoreduced temperatures T_R' and the available low-pressure data. Thermal-conductivity ratios calculated with this value were plotted on Figure 2 and were found to be consistent with the ratios for the other inert gases only in the reduced temperature range above $T_R = 3.0$.

Figure 3 is presented as an alternative correlation to Figure 2. This plot was prepared by calculating the k^* and $k_{T_c}^*$ values directly from Equation (1). The straight-line portions of the curve are given by the expressions

$$\frac{k^*}{k_{T_c}^*} = T_R \quad \text{for} \quad T_R \leq 1.0 \qquad (13)$$

$$\frac{k^*}{k_{T_c}^*} = 1.276 T_R^{0.645} \quad \text{for} \quad T_R \geq 3.5 \qquad (14)$$

Thermal conductivities obtained from Figure 3 are in good agreement with the experimental values. However, Figure 2 is somewhat more accurate since this was produced directly from experimental data.

Equation (8) can be expressed in the form

$$\log \frac{k^*}{k_c} = B \log T_R + \log \frac{1}{A} \qquad (15)$$

where $A = (k_c/C)$ and is a constant characteristic of a given family of substances. At a reduced temperature of $T_R = 1.0$, Equation (15) simplifies to the following relationship defining the thermal conductivity of a substance at the critical point:

$$k_c = A k_{T_c}^* \qquad (16)$$

The constant A of Equation (16) can be evaluated if a single thermal-conductivity value can be determined at the critical point and if a corresponding $k_{T_c}^*$ value can be established. Ordinarily, low-pressure thermal conductivities can be obtained from the literature; and values at the critical temperature $k_{T_c}^*$ can be determined either directly or by extrapolation. However, if the experimental data for a substance are limited, $k_{T_c}^*$ can be produced directly from a single thermal-conductivity measurement and a relationship of the type presented in Figure 2. With Equation (16) it is then possible to calculate the critical thermal conductivity k_c for each member of a family having an established value of $k_{T_c}^*$.

A reliable value for the critical thermal conductivity of argon was obtained by using an equation of the form originally proposed by Abas-Zade (*1*):

$$k - k^* = a\rho^b \qquad (17)$$

where k and ρ represent the thermal conductivity and density, respectively, at any temperature and pressure and k^* is evaluated at a low pressure* and the same temperature. In Equation (17) the quantity a is a constant, and the exponent b is a function of density only.

The experimental data available for argon were used to calculate the residual thermal conductivities $k - k^*$. These values were correlated with experimental densities ρ (*17, 20, 30, 36*) according to

---

*A condition where P_R is essentially equal to zero.

Equation (17) to produce the curve presented in Figure 4. It is important to note that the experimental data defined a single, continuous curve for both the gaseous and liquid states and that this function appears to be independent of temperature and pressure as indicated by Equation (17).

The relationship of Figure 4 possesses a number of distinct advantages over previous methods of correlation. For its complete definition, this plot requires only a moderate amount of reliable liquid and high-pressure gaseous-state data. Once established, the correlation defines thermal-conductivity values for all conditions of temperature and pressure corresponding to the entire range of densities plotted on the curve. Consequently, it is also possible to calculate the critical thermal conductivity of a substance k_c directly from the critical density and the corresponding $k_{T_c}{}^*$ value.

Through this approach the critical thermal conductivity of argon was established directly from the density at the critical point and the $k_{T_c}{}^*$ value obtained from Figure 1. Specifically, the critical thermal conductivity for argon was calculated to be $k_c = 7.10 \times 10^{-5}$ cal./(sec.)(cm.)(°K.) from a value of $k_{T_c}{}^* = 2.33 \times 10^{-5}$ and a residual thermal conductivity, $k - k^* = 4.77 \times 10^{-5}$ obtained from Figure 4 at a critical density, $\rho_c = 0.531$ g./cu. cm.

By use of the critical thermal conductivity for argon, the constant of Equation (16) was calculated to be $A = 3.047$. Therefore, for the inert-gas family, Equation (16) becomes

$$k_c = 3.047 k_{T_c}{}^* \qquad (18)$$

Critical thermal conductivities for helium, neon, krypton, and xenon were calculated from Equation (18) with the $k_{T_c}{}^*$ values presented in Figure 2. The resulting critical values for all the inert gases are as follows:

	k_c, cal./(sec.)(cm.)(°K.)
Helium	14.62×10^{-5}
Neon	7.92
Argon	7.10
Krypton	4.92
Xenon	4.02
Radon*	3.12

---

*Calculated from Equation (20).

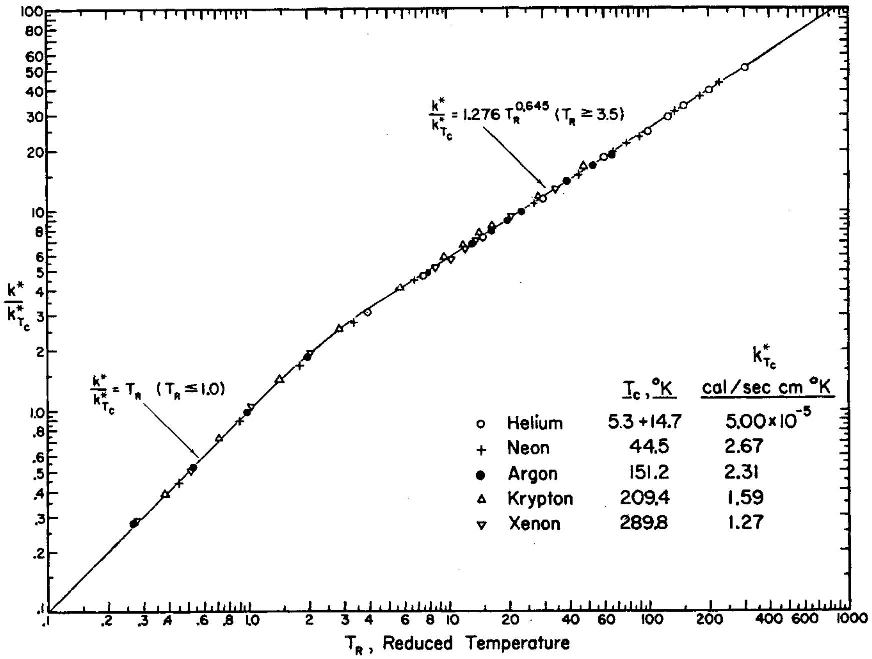

Fig. 3. Thermal-conductivity ratios for the inert gases (reference state: $T_R = 1.0$, $P_R = 0$) (points calculated with the Hirschfelder, Curtiss, and Bird equation).

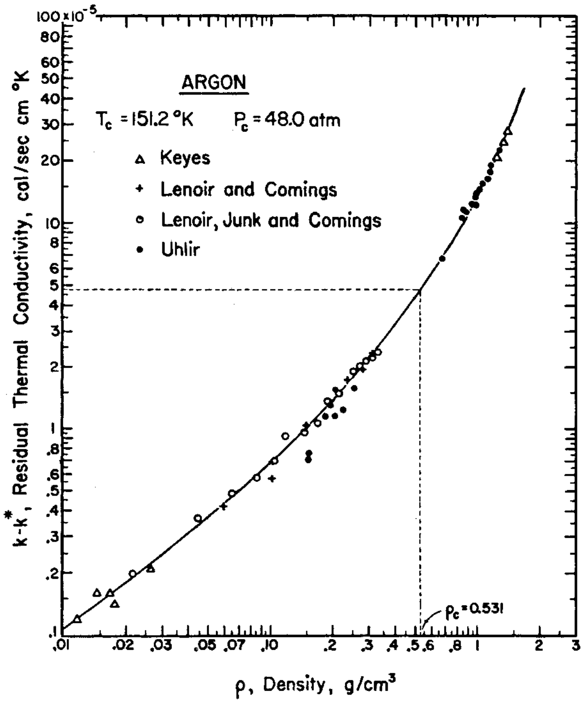

Fig. 4. Relationship of residual thermal conductivity and density for argon in the gaseous and liquid states.

The critical-temperature correction necessary to make the correlation of helium consistent with that of the other inert gases has been given previously as 14.7°K., but since high-pressure thermal-conductivity data for helium are limited, a proper correction for the critical pressure is difficult to establish. In order to obtain such a value, an equation of the form (*50*)

$$k_c = d M^e T_c{}^f P_c{}^g \qquad (19)$$

was assumed to apply for all the inert gases. The critical values for neon, argon, krypton, and xenon were used to evaluate the constants of Equation (19), and this equation thereby becomes

$$k_c = 13.39 \times 10^{-5} \frac{P_c{}^{0.223} T_c{}^{0.132}}{M^{0.586}} \qquad (20)$$

From the values $k_c = 14.62 \times 10^{-5}$ cal./(sec.)(cm.)(°K.), $T_c' = 20$°K., and $M = 4.003$, the pseudocritical pressure for helium was calculated from Equation (20) as 9.60 atm. This value requires that a correction of 7.34 atm. be added to the actual critical pressure.

It is logical to assume that Equation

(20) is also applicable to radon, which has the following characteristic constants (*30*): $M = 222$, $T_c = 377.6°\text{K.}$, $P_c = 62.44$ atm. With these values used in Equation (20), the critical thermal conductivity for radon was calculated to be $k_c = 3.12 \times 10^{-5}$ cal./(sec.)(cm.)(°K.).

CONSTRUCTION OF REDUCED-STATE CORRELATION

Reduced thermal conductivities were calculated for the inert gases by use of all the experimental data available in the literature and the critical constants presented above. These values were plotted against reduced temperature on log-log scales to produce the correlation presented as Figure 5. An examination of this figure indicates that the data for helium, neon, argon, krypton, and xenon all follow a corresponding-states behavior. However, it is apparent that the available data are fragmentary and limited to a few particular regions of temperature and pressure.

In order to extend the range of Figure 5, it was necessary to define the density of argon over the entire region of temperature and pressure required for the final reduced-state correlation. To provide these values, Figure 6 was constructed on the basis of the experimental densities reported in the literature (*17, 20, 30, 36*). For conditions where no experimental data were available, density values were calculated. In the gaseous-state region the compressibility factors of Nelson and Obert (*38*) were used to apply a temperature correction to existing high-pressure data (*36*). To obtain liquid-state values, saturated liquid densities were corrected for pressure effects by means of the ω factors proposed by Watson (*57*). At pressures above $P_R = 5$ it was necessary to extrapolate the gaseous-state isobars into the liquid region.

Figure 7 presents the final reduced-state correlation for the inert gases. In this figure the low-pressure curve $P_R = 0$ was established directly from the corresponding data presented in Figure 5. The construction of the remaining curves was based on the correlations for argon given in Figures 1, 4, and 6.

Each isobar was defined by first selecting a number of density values covering the entire range of desired temperatures for a fixed pressure. A residual thermal conductivity $k - k^*$ corresponding to each density was then obtained from Figure 4. With the proper value of k^* from Figure 1, thermal conductivities were established for the selected temperatures and constant pressure. Reduced thermal conductivities were calculated from these values and then plotted in Figure 7. Isobars constructed in this manner extend up to reduced pressures of 40 and cover a reduced temperature range from 0.1 to 100.

TABLE 2. COMPARISON OF THERMAL CONDUCTIVITIES CALCULATED FROM FIGURE 7 WITH EXPERIMENTAL VALUES FOR THE INERT GASES

	Low-pressure region			Liquid and high-pressure gaseous region					Combined
	Experimental Points	% Deviation Maximum	% Deviation Average	Experimental Points	% Deviation Maximum	% Deviation Average	Range investigated T_R	Range investigated P_R	average % deviation†
Helium*	34	5.2	1.4	8	1.3	0.8	3.8–48	0–21.4	1.2
Neon	17	2.3	0.6	—	—	—	2 –13	0	0.6
Argon	25	3.7	1.2	96	10.7	2.3	0.57– 6.4	0– 4.5	2.1
Krypton	8	2.9	1.2	9	4.3	2.0	0.59– 2.8	0– 0.2	1.6
Xenon	8	3.0	1.9	7	5.7	4.2	0.5 – 2.0	0– 0.18	3.0

The over-all % deviation for the monoatomic gases is 1.8%.

*The reduced-state plot of Figure 7 applies for helium only in the reduced temperature range above $T_R = 3.0$, therefore for helium no comparisons are included for the liquid region or for the gaseous region below $T_R = 3.0$,

†% Deviation $= \dfrac{k_{calc.} - k_{exp.}}{k_{exp.}} \times 100$.

NORMALIZED-STATE CORRELATION

The thermal-conductivity values from Figure 7 were replotted with new reference states to produce the normalized plot of Figure 8. This correlation is based on the theorem of corresponding states expressed in terms of molecular properties and intermolecular forces rather than critical constants. The variables in Figure 8 are dimensionless factors defined analytically as follows:

$$T_N = \frac{T}{\epsilon/\kappa} \tag{21}$$

$$P_N = \frac{P}{\epsilon/\sigma^3} \tag{22}$$

$$k_N = \frac{k}{\dfrac{\kappa}{\sigma^2}\sqrt{\dfrac{\epsilon N}{M}}} \tag{23}$$

These normalized quantities are derived on the assumption that the intermolecular forces between two molecules of a pure gas follow the Lennard-Jones potential-energy function given by the equation

$$\varphi(r) = 4\epsilon\left[\left(\frac{\sigma}{r}\right)^{12} - \left(\frac{\sigma}{r}\right)^{6}\right] \tag{24}$$

It should be noted that ϵ and σ in Equation (24) are characteristic constants for each specific substance and are combined with the appropriate molecular constants to provide a basis for the dimensionless normalized temperature, pressure, and thermal conductivity defined by Equations (21), (22), and (23). The ϵ and σ values given in Figure 8 were obtained from Hirschfelder, Curtiss, and Bird (*14*).

The normalized plot presented in Figure 8 is convenient because it requires only values of ϵ and σ and the molecular

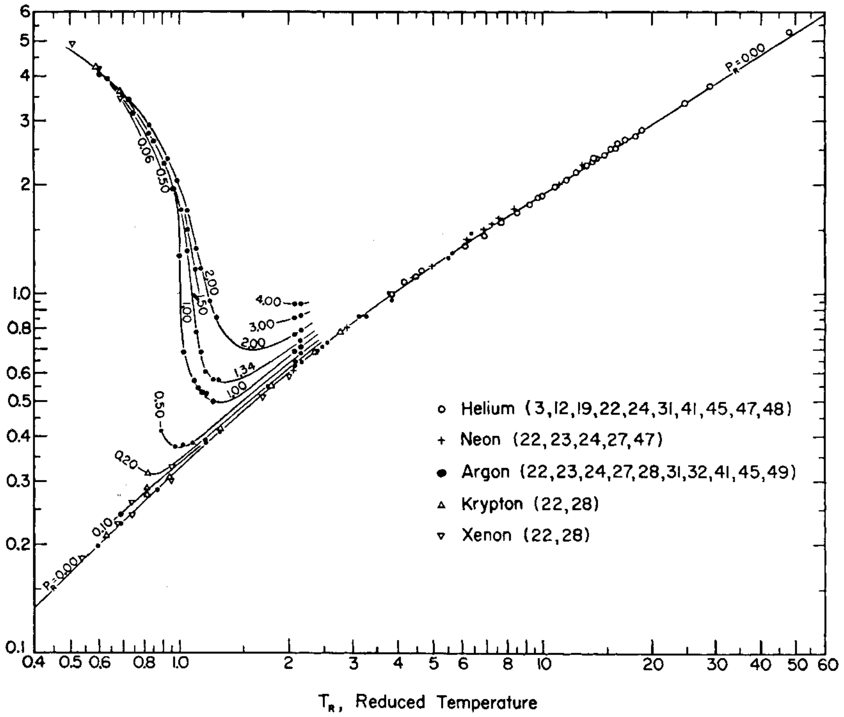

Fig. 5. Reduced-state plot of thermal-conductivity data obtained from the literature.

TABLE 3. COMPARISON OF THERMAL CONDUCTIVITIES CALCULATED FROM FIGURE 7 WITH SELECTED EXPERIMENTAL VALUES FOR SOME DIATOMIC, TRIATOMIC, AND HYDROCARBON GASES

	k_c, cal./(sec.)(cm.)(°K.)	Range investigated T_R	Range investigated P_R	Experimental points	% Deviation Maximum	% Deviation Average	References
Diatomic							
Hydrogen*	50.6×10^{-5}	0.85–7.1	0	13	12.3	4.3	*4, 19, 27, 53*
Nitrogen	8.68	0.54–8.5	0–38.5	126	8.4	2.6	*10, 26, 31, 32, 35, 40, 41, 49*
Oxygen†	10.53	0.55–5.1	0–1.9	19	37.4	7.4	*2, 10, 28*
Carbon monoxide	8.65	0.66–2.8	0	10	7.2	2.4	*19*
Nitric oxide	11.82	0.72–2.1	0	8	3.1	1.0	*19*
Chlorine	9.70	0.48–1.6	0	7	16.0	5.6	*10*
Hydrogen chloride	11.30	0.61–1.78	0	5	6.0	3.4	*10*
Triatomic							
Carbon dioxide	12.2	0.66–2.1	0–2.8	15	29.2	11.6	*19, 26, 31*
Nitrous oxide	13.1	0.61–1.2	0	5	22.0	10.4	*19*
Sulfur dioxide	9.86	0.64–0.68	0	4	2.6	1.3	*9*
Water	33.4	0.58–0.96	0–0.69	9	13.8	5.8	*29*
Hydrocarbons							
Methane	15.8	0.51–2.0	0–4.4	16	16.1	6.5	*19, 28, 32*
Ethane	20.3	1.0 –1.4	0–4.1	13	119	32.0	*32, 55*

---

*For hydrogen the reduced-state plot of Figure 7 applies only for the isobar $P_R = 0$, for which a corrected critical temperature of 100°K. must be used.

†For oxygen the experimental data include four points in the liquid region which produce large deviations. If these points are not considered, the average deviation for oxygen is 2.7% with a maximum of 6.8%.

weight; all of which can be obtained from the literature or can be evaluated from experimental viscosity data (*14*). No knowledge of the critical temperature, pressure, or thermal conductivity is necessary. However, because of the assumptions made in the theoretical development of this approach, this correlation should be restricted to monoatomic gases. Figure 8 is comparable to Figure 7 and is presented for completeness in view of the novelty of these concepts defining the reference states of transport properties from statistical and quantum mechanic approaches.

DISCUSSION OF RESULTS

The accuracy of the correlation presented in Figure 7 has been checked with the original experimental data taken from the literature sources given in Table 1, and the results of these comparisons are presented in Table 2. It is significant that the over-all deviation of the inert gases is only 1.8% for the 212 experimental points considered. Furthermore, it is observed that the liquid and the high-pressure gaseous regions of Figure 7 are accurate for all the inert gases despite the fact that these general areas were developed only from data for argon. It should be emphasized, however, that this figure is applicable to helium only in the gaseous state for reduced temperatures above $T_R = 3$.

The correlation of Figure 7 has been checked for generality by comparing the results for some diatomic, triatomic, and hydrocarbon gases with experimental values obtained from the literature. Table 3 presents a summary of these comparisons. The calculated deviations indicate that Figure 7 produces reliable thermal conductivities for the diatomic gases; however, it appears that significant errors are encountered for substances having more than two atoms per molecule such as carbon dioxide, nitrous oxide, methane, and ethane.

To make the evaluation of Table 3, it was necessary to calculate an average k_c for each substance by dividing reduced thermal conductivities from Figure 7 into experimental k values and averaging the resulting k_c values. The critical constants obtained in this manner may not necessarily represent the true thermal conductivity at the critical point and therefore should be used only with Figure 7.

Experimental data for a number of mixtures have also been considered from the standpoint of the pseudocritical concept. Critical properties for each mixture were calculated from the following equations:

$$T_c' = \sum_i N_i T_{ci} \qquad (25)$$

$$k_c' = \sum_i N_i k_{ci} \qquad (26)$$

From the comparisons presented in Table 4, it appears that Figure 7 is generally applicable to mixtures of both mono- and diatomic gases including air. However, these comparisons are limited to the low-pressure region, as no high-

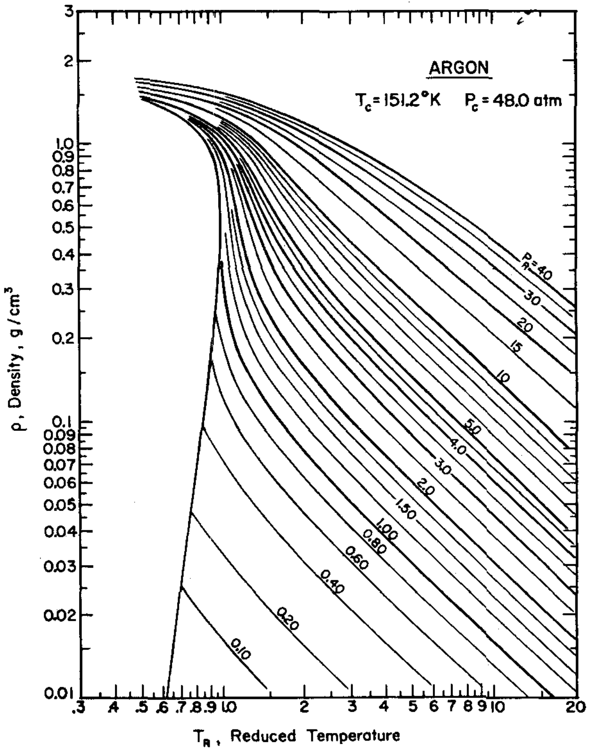

Fig. 6. Density chart for argon in the gaseous and liquid states.

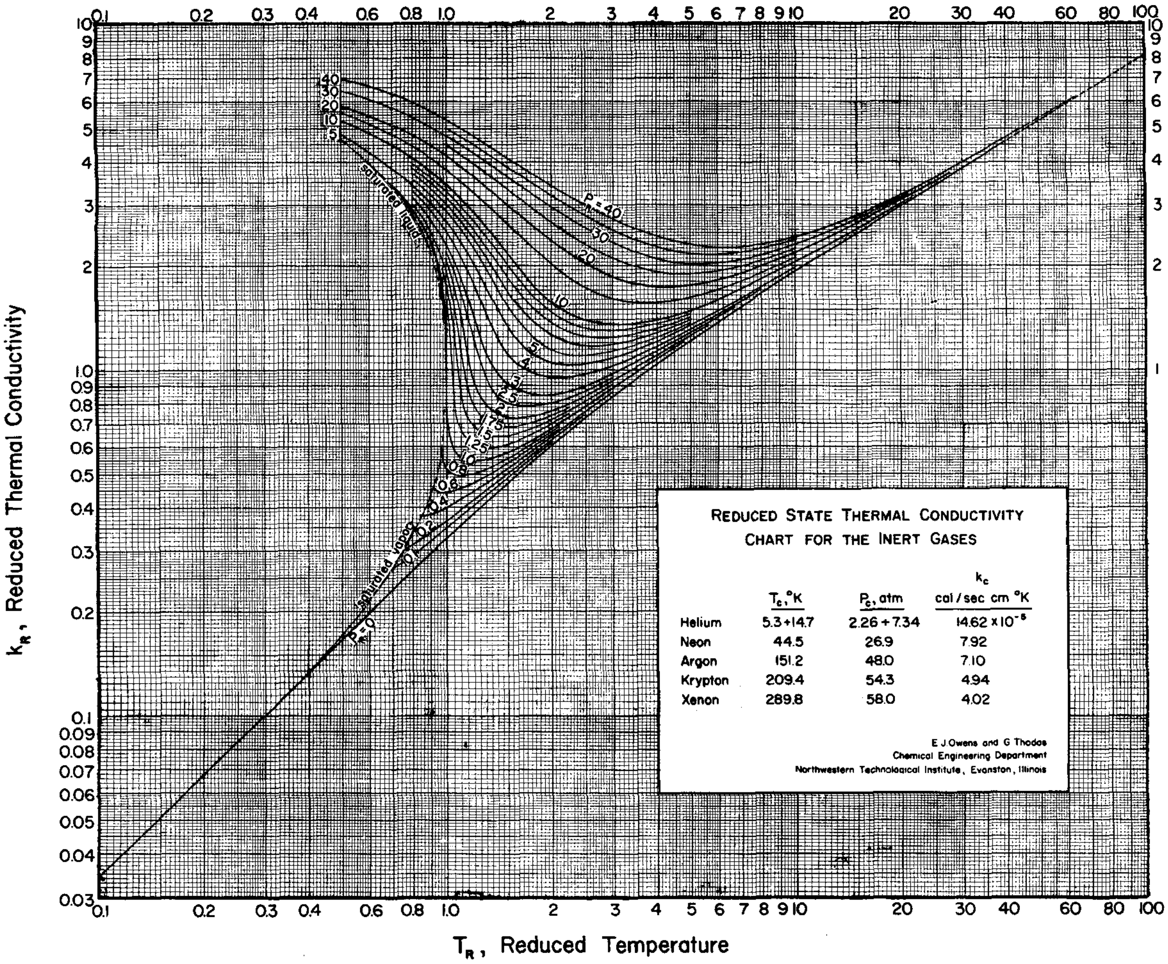

REDUCED STATE THERMAL CONDUCTIVITY
CHART FOR THE INERT GASES

	T_c, °K	P_c, atm	k_c cal / sec cm °K
Helium	5.3+14.7	2.26+7.34	14.62 × 10^{-6}
Neon	44.5	26.9	7.92
Argon	151.2	48.0	7.10
Krypton	209.4	54.3	4.94
Xenon	289.8	58.0	4.02

E J Owens and G Thodos
Chemical Engineering Department
Northwestern Technological Institute, Evanston, Illinois

Fig. 7. Reduced-state plot of thermal conductivity for the inert gases.

pressure data for mono- or diatomic gas mixtures are available in the literature.

Since Figure 8 contains the same basic data as given in Figure 7, only a moderate number of comparisons were made to determine the accuracy and limitations of the normalized plot relative to the reduced-state correlation. Based on more than fifty randomly selected experimental values, thermal conductivities calculated from Figure 8 produced an average deviation of about 1% for the inert gases. In these comparisons the data for helium were found to be in excellent agreement with those of the other inert gases for normalized temperatures above $T_N = 2.5$. For helium no correction was required on the original molecular parameters to produce this good agreement.

CONCLUSIONS

The validity of the general correlation method developed in this study is substantiated by the results for the inert gases presented in Table 2. It is important to emphasize that this method requires only a moderate amount of reliable liquid- and high-pressure-gaseous-state data in order to produce an extensive reduced-state correlation of the form given in Figure 7. Also, it is apparent that the proposed procedure should be applicable to any family of similar fluids since it is limited only by the assumption of a corresponding-states behavior.

ACKNOWLEDGMENT

The authors gratefully acknowledge the fellowship grant provided by the Dow Chemical Company which made this study possible.

TABLE 4. COMPARISON OF THERMAL CONDUCTIVITIES CALCULATED FROM FIGURE 7 WITH EXPERIMENTAL VALUES FOR SOME GASEOUS MIXTURES AT LOW PRESSURES

System	Mole Fraction	Temp., °K.	Maximum	Average	References
Helium-argon	He = 0.270, 0.454, 0.847, 0.946	273	14.5	8.7	*56*
Nitrogen-argon	N_2 = 0.204, 0.359, 0.611, 0.780	273	1.9	1.1	*58*
Air*	— — — —	90-873	6.3	1.9	*21, 44, 52*
Carbon monoxide-air	CO = 0.108, 0.321, 0.562, 0.978	291	5.6	5.0	*13*

---

*The pseudocritical constants for air were calculated to be $T_c' = 132.2$ °K. and $k_c' = 9.08 \times 10^{-5}$ cal./(sec.)(cm.)(°K.). A total of 14 experimental points were used to calculate the % deviation.

NOTATION

a = constant
A = constant as defined by Equation (16)
b = function of density
B = function of reduced temperature
C = constant
d, e, f, g = constants for Equation (19)
f_k = thermal-conductivity correction factor to dilute gases for Equation (1)
k = thermal conductivity at any temperature and pressure
k^* = thermal conductivity at low pressures (P_R essentially equal to zero)
$k_{T_c}^*$ = thermal conductivity at low pressures and the critical temperature
k_c = thermal conductivity at the critical point
k_c' = pseudocritical thermal conductivity
k_N = normalized thermal conductivity,

$$\frac{k}{\frac{\kappa}{\sigma^2}\sqrt{\frac{\epsilon N}{M}}}$$

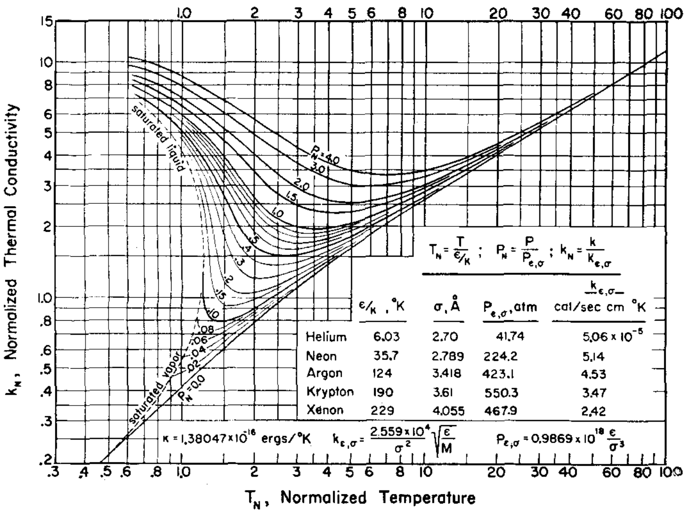

$T_N = \frac{T}{\epsilon/\kappa}$; $P_N = \frac{P}{P_{\epsilon,\sigma}}$; $k_N = \frac{k}{k_{\epsilon,\sigma}}$

	ϵ/κ, °K	σ, Å	$P_{\epsilon,\sigma}$, atm	$k_{\epsilon,\sigma}$ cal/sec cm °K
Helium	6.03	2.70	41.74	5.06×10^{-5}
Neon	35.7	2.789	224.2	5.14
Argon	124	3.418	423.1	4.53
Krypton	190	3.61	550.3	3.47
Xenon	229	4.055	467.9	2.42

$\kappa = 1.38047 \times 10^{-16}$ ergs/°K $k_{\epsilon,\sigma} = \frac{2.559 \times 10^4}{\sigma^2}\sqrt{\frac{\epsilon}{M}}$ $P_{\epsilon,\sigma} = 0.9869 \times 10^{18} \frac{\epsilon}{\sigma^3}$

Fig. 8. Normalized thermal-conductivity correlation for the inert gases (after Hirschfelder, Curtiss, and Bird method).

k_R = reduced thermal conductivity, k/k_c
k_R^* = reduced thermal conductivity at low pressures, k^*/k_c
M = molecular weight
N = Avogadro number, 6.0228×10^{23} molecules/gram-mole
N_i = mole fraction of ith component
P = absolute pressure, atm.
P_c = critical pressure, atm.
P_c' = pseudocritical pressure, atm.
P_N = normalized pressure, $P/\epsilon/\sigma^3$
P_R = reduced pressure, P/P_c
r = intermolecular distance, Å.
R = gas constant
T = absolute temperature, °K.
T_c = critical temperature, °K.
T_c' = pseudocritical temperature, °K.
T_N = normalized temperature, $T/\epsilon/\kappa$
T_R = reduced temperature, T/T_c
T_R' = pseudoreduced temperature, T/T_c'

Greek Letters

α = constant for Equation (2)
β = molecular volume
ϵ = maximum energy of attraction between two gas molecules at low pressures, ergs
κ = Boltzmann constant, 1.38047×10^{-16} ergs/°K.
μ = viscosity
μ^* = viscosity at low pressures
μ_c = viscosity at the critical point
μ_R = reduced viscosity, μ/μ_c
μ_R^* = reduced viscosity at low pressures, μ^*/μ_c
ρ = density, g./cc.
ρ_c = critical density, g./cc.
σ = distance between centers of two colliding gas molecules, Å.
$\varphi(r)$ = Lennard-Jones potential-energy function
χ = collision frequency factor
ω = expansion factor for the liquid state
$\Omega^{(2,2)*}[T_N]$ = Lennard-Jones transport-property function

LITERATURE CITED

1. Abas-Zade, A. K., *Zhur. Eksptl. Teort. Fiz.*, **23**, 60 (1952).
2. Borovik, E., *ibid.*, **17**, 328 (1947).
3. Bowers, R., *Proc. Phys. Soc. (London)*, **65A**, 511 (1952).
4. Bromley, L. A., *U. S. Atomic Energy Comm. Tech. Inform. Service UCRL-1852* (1952).
5. Chow, W. M., and J. A. Bright, Jr., *Chem. Eng. Progr.*, **49**, 175 (1953).
6. de Boer, J., and R. J. Lunbeck, *Physica*, **14**, 520 (1948).
7. Enskog, David, *Kgl. Svenska Vetenskapsakad. Handl.*, **63**, No. 4 (1922).
8. Eucken, A., *Forsch. Gebiete Ingenieurw.*, **11B**, 6 (1940).
9. Foz Gazulla, O. R., and S. S. Perez, *Anales fíz. y quím. (Madrid)*, **39**, 399 (1943).
10. Franck, E. U., *Z. Elektrochem.*, **55**, 636 (1951).
11. Gamson, B. W., *Chem. Eng. Progr.*, **45**, 154 (1949).
12. Grenier, C., *Phys. Rev.*, **83**, 598 (1951).
13. Gruss, H., and H. Schmick, *Wiss. Veröffentl. Siemens-Konzern*, **7**, 202 (1928).
14. Hirschfelder, J. O., C. F. Curtiss, and R. B. Bird, "Molecular Theory of Gases and Liquids," pp. 534–578, John Wiley and Sons, New York (1954).
15. *Ibid.*, pp. 633–634.
16. *Ibid.*, pp. 634–652.
17. Holburn, L., H. Schultze, and J. Otto, "*Handbuch der Experimentalphysik*, Vol. VIII, p. 152, Leipzig Akademische Verlagsgessellschaft, M. B. H. (1929).
18. Hougen, O. A., and K. M. Watson, "Chemical Process Principles," pp. 479–535, John Wiley and Sons, New York (1947).
19. Johnston, H. L., and E. R. Grilly, *J. Chem. Phys.*, **14**, 233 (1946).
20. Kamerlingh Onnes, H., and C. A. Crommelin, *Communs. Phys. Lab., Univ. Leiden*, No. 118b (1910).
21. Kannuluik, W. G., and E. H. Carman, *Australian J. Sci. Research*, **A4**, 305 (1951).
22. ———, *Proc. Phys. Soc. (London)*, **65B**, 701 (1952).
23. Kannuluik, W. G., and H. B. Donald, *Australian J. Sci. Research*, **A3**, 417 (1950).
24. Kannuluik, W. G., and L. H. Martin, *Proc. Roy. Soc. (London)*, **A144**, 496 (1934).
25. Keyes, F. G., *Trans. Am. Soc. Mech. Engrs.*, **73**, 589 (1951).
26. *Ibid.*, 597.
27. *Ibid.*, **76**, 809 (1954).
28. *Ibid.*, **77**, 1395 (1955).
29. ———, and D. J. Sandell, Jr., *Ibid.*, **72**, 767 (1950).
30. Lange, N. A., "Handbook of Chemistry," 7 ed., pp. 1458, 1464, Handbook Publishers, Inc., Sandusky, Ohio (1949).
31. Lenoir, J. M., and E. W. Comings, *Chem. Eng. Progr.*, **47**, 223 (1951).
32. Lenoir, J. M., W. A. Junk, and E. W. Comings, *ibid.*, **49**, 539 (1953).
33. Maslan, F. D., and T. M. Littman, *Ind. Eng. Chem.*, **45**, 1566 (1953).
34. Maxwell, J. C., "Collected Works," Vol. II, p. 1, Cambridge University Press, London (1890).
35. Michels, A., and A. Botzen, *Physica*, **19**, 585 (1953).
36. Michels, A., Hub Wijker, and Hk. Wijker, *ibid.*, **15**, 627 (1949).
37. Nathan, M. F., and E. W. Comings, *Ind. Eng. Chem.*, **39**, 964 (1947).
38. Nelson, L. C., and E. F. Obert, *Trans. Am. Soc. Mech. Engrs.*, **76**, 1057 (1954).
39. Owens, E. J., M.S. thesis, Northwestern Univ., Evanston, Ill. (1956).
40. Powers, R. W., R. W. Mattox, and H. L. Johnston, *J. Am. Chem. Soc.*, **76**, 5968 (1954).
41. Rothman, A. J., *U. S. Atomic Energy Comm., Tech. Inform. Service UCRL-2339* (1954).
42. Sakiadis, B. C., and Jesse Coates, *A.I.Ch.E. Journal*, **1**, 275 (1955).
43. *Ibid.*, **2**, 88 (1956).
44. Schmidt, A. F., and B. H. Spurlock, Jr., *Trans. Am. Soc. Mech. Engrs.*, **76**, 823 (1954).
45. Soddy, F., and A. J. Berry, *Proc. Roy. Soc. (London)*, **A84**, 576 (1911).
46. Sutherland, William, *Phil. Mag.*, **40**, 421 (1895).
47. Thomas, L. B., and R. C. Golike, *J. Chem. Phys.*, **22**, 300 (1954).
48. Ubbink, J. B., and W. J. de Haas, *Physica*, **10**, 465 (1943).
49. Uhlir, A., Jr., *J. Chem. Phys.*, **20**, 463 (1952).
50. Uyehara, O. A., and K. M. Watson, *Natl. Petroleum News, Tech. Sec.*, **36**, R764 (Oct. 4, 1944).
51. van der Waals, J. D., *Beibl. Ann. Physik*, **5**, 250 (1881).
52. Vargaftik, N. B., and O. A. Oleshchuk, *Izvest. V.T.I.*, **15**, No. 6, 7 (1946).
53. Vargaftik, N. B., and I. D. Parfenov, *J. Exptl. Theoret. Phys. (U.S.S.R.)*, **8**, 189 (1938).
54. Vines, R. G., *Australian J. Chem.*, **6**, 1 (1953).
55. ———, and L. A. Bennett, *J. Chem. Phys.*, **22**, 360 (1954).
56. Wachsmuth, J., *Physik. Z.*, **9**, 235 (1908).
57. Watson, K. M., *Ind. Eng. Chem.*, **35**, 398 (1943).
58. Weber, S., *Ann. Physik*, **54**, 481 (1917).